AMERICAN SOCIETY FOR MICROBIOLOGY | Molecular and Cellular Biology®

RESEARCH ARTICLE

Predicted RNA Binding Proteins Pes4 and Mip6 Regulate mRNA Levels, Translation, and Localization during Sporulation in Budding Yeast

Liang Jin, Kai Zhang, Rolf Sternglanz, Aaron M. Neiman

Department of Biochemistry and Cell Biology, Stony Brook University, Stony Brook, New York, USA

ABSTRACT In response to starvation, diploid cells of *Saccharomyces cerevisiae* undergo meiosis and form haploid spores, a process collectively referred to as sporulation. The differentiation into spores requires extensive changes in gene expression. The transcriptional activator Ndt80 is a central regulator of this process, which controls many genes essential for sporulation. Ndt80 induces ~300 genes coordinately during meiotic prophase, but different mRNAs within the *NDT80* regulon are translated at different times during sporulation. The protein kinase Ime2 and RNA binding protein Rim4 are general regulators of meiotic translational delay, but how differential timing of individual transcripts is achieved was not known. This report describes the characterization of two related *NDT80*-induced genes, *PES4* and *MIP6*, encoding predicted RNA binding proteins. These genes are necessary to regulate the steady-state expression, translational timing, and localization of a set of mRNAs that are transcribed by *NDT80* but not translated until the end of meiosis II. Mutations in the predicted RNA binding domains within *PES4* alter the stability of target mRNAs. *PES4* and *MIP6* affect only a small portion of the *NDT80* regulon, indicating that they act as modulators of the general Ime2/Rim4 pathway for specific transcripts.

KEYWORDS RRM domain, mRNA localization, mRNA stability, sporulation, translational control

Received 12 July 2016 **Returned for modification** 16 August 2016 **Accepted** 5 February 2017

Accepted manuscript posted online 13 February 2017

Citation Jin L, Zhang K, Sternglanz R, Neiman AM. 2017. Predicted RNA binding proteins Pes4 and Mip6 regulate mRNA levels, translation, and localization during sporulation in budding yeast. Mol Cell Biol 37:e00408-16. https://doi.org/10.1128/MCB.00408-16.

Address correspondence to Aaron M. Neiman, aaron.neiman@stonybrook.edu.

Starvation for nitrogen in the presence of a poor carbon source triggers the differentiation of diploid baker's yeast into haploid ascospores (1). In this process, the cell first undergoes premeiotic S phase, recombination and synapsis during meiotic prophase, and two meiotic divisions. The formation of spores begins during the second meiotic division, when secretory vesicles coalesce to form novel intracellular compartments termed prospore membranes (2). Each of the four daughter nuclei is engulfed by prospore membranes, and enclosure of the prospore membrane at the end of meiosis II creates distinct daughter cells. These daughter cells mature into spores by the deposition of a wall material around each newly formed spore (3).

A well-characterized transcriptional cascade drives this differentiation process (1). Starvation induces the expression of the *IME1* gene (4, 5). *IME1* then activates transcription of many of the genes involved in the events of meiotic prophase, including the protein kinase gene *IME2* (5). *IME1* and *IME2* together promote expression of the meiosis-specific transcription factor gene *NDT80* (6–8). Ndt80 induces the expression of about 300 genes, referred to as the "*NDT80* regulon" (9). Included in the *NDT80* regulon are genes involved in different events of meiosis and spore formation. For instance, Ndt80 induces expression of *CDC5*, required for completion of meiotic recombination, the *CLB* genes necessary to drive the nuclear divisions of meiosis, *SPO20* and other genes involved in formation and growth of prospore membranes, and genes involved in the later steps of spore wall assembly (2, 10–12). The transcriptional timing of the

NDT80 regulon presented a paradox in that expression of all of these genes is induced with similar kinetics and yet the different events that they promote occur over a period of ~3 h.

Ribosome profiling of a meiotic time course revealed the answer to this paradox: while the mRNAs of the *NDT80* regulon are coordinately transcribed, their translational timing is distinct (13). Many of the messages are translated as soon as they are induced. Another portion, including genes such as *CLB3* and *SPO20*, are delayed in translation until the onset of meiosis II (10, 13). For others, their peak translation is delayed until the end of meiosis II (13). Thus, upon induction of *NDT80*, the fine timing of gene expression shifts from transcriptional to translational control.

Differential translational timing is controlled by a regulatory circuit involving the RNA binding protein Rim4 and the protein kinase Ime2 (14). Rim4 binds to the 5′ untranslated region (UTR) of the *CLB3* message, and mutations in the Rim4 RNA binding domain result in early translation of *CLB3* (14). Ime2 activity is high in premeiotic S phase and then drops as cells exit meiotic prophase and rises again as cells progress through the meiotic divisions (6). Phosphorylation of Rim4 by Ime2 destabilizes the Rim4 protein, and mutations that hyperactivate Ime2 also cause early translation of *CLB3* (14). These results support a model in which Ime2 negatively regulates Rim4, which is itself an inhibitor of translation (14). In addition to *CLB3* translation, *IME2* and *RIM4* also control the translation of *SPS4*, which is translated at the end of meiosis II (15).

While *IME2* and *RIM4* appear to be global regulators of translational timing in meiosis, how the distinct timing of translation of different transcripts is achieved is not understood. *SPS4* is one of a set of 19 genes whose translation is delayed until the end of the meiotic divisions (13). In addition to this long translational delay, these transcripts also display a phenomenon termed "protection" (15). When cells in meiosis II are returned to rich medium, most of the transcripts in the *NDT80* regulon are unstable and their levels drop significantly (15, 16). However, for protected transcripts, the mRNA levels remain stable. Protection correlates both with translation at the end of meiosis II and with the localization of these transcripts to discrete foci (15). Neither protection nor focal localization is seen for transcripts like *SPO20* that are translated at the end of meiosis I. All three properties, late translation, protection, and focal localization, are lost in cells carrying hyperactive *IME2* (15). These observations suggest that sequestration of transcripts like *SPS4* in foci confers on them both the protection and the additional temporal delay that distinguishes them from the *CLB3* class of transcripts with delayed translation (15). Rim4 associates with both *CLB3* and *SPS4* class transcripts (14) and therefore cannot alone account for the behavior of *SPS4* class messages. One explanation for the protection and delayed translation of *SPS4* class transcripts is the presence of additional factors responsible for organizing the transcripts in foci.

This report describes the identification of two predicted RNA binding proteins, Pes4 and Mip6, as regulators of late translation, protection, and mRNA localization. *PES4* and *MIP6* are themselves induced by *NDT80* and translated early. Thus, *NDT80* induces expression of genes that then delay translation of other portions of the regulon. This regulatory logic appears to be conserved in gametogenesis in other organisms as well.

RESULTS

***PES4* and *MIP6* have redundant functions in spore formation.** Association with Rim4 is not sufficient to explain how differential translational timing of different transcripts is regulated, suggesting that additional RNA binding proteins might be needed (15). The *NDT80* regulon was examined for proteins that might be implicated in translational control. Two *NDT80*-induced genes, *PES4* and *MIP6*, encode proteins that each contain three RNA recognition motif (RRM) domains, which are 90-amino-acid domains found in a large number of RNA binding proteins (17). *PES4* and *MIP6* encode paralogs with ~40% sequence identity (18, 19). Deletion of *MIP6* does not have any detectable mutant phenotypes, while *PES4* has been implicated in the formation of the outer spore wall (20). To test whether *PES4* and *MIP6* share any functions involved in

sporulation, isogenic single and double mutant diploids were constructed (Table 1) and sporulation was examined (Fig. 1). Both *pes4*Δ and *mip6*Δ single mutants displayed wild-type (WT) levels of sporulation. Furthermore, the distribution of ascal types was similar to the wild type in that predominantly four-spored asci (tetrads) were seen. In contrast, the *pes4*Δ *mip6*Δ double mutant exhibited a 2-fold increase in the number of unsporulated cells (Fig. 1). For those cells that did make spores, there was an increase in the number of asci containing only one, two, or three spores with a corresponding decrease in tetrads. The spores that did form in the *pes4*Δ *mip6*Δ mutant were 95% viable (50 tetrads dissected) and showed no obvious sensitivity to ether, suggesting that the double mutant does not have significant spore wall defects (L. Jin, unpublished observations). Nonetheless, these results demonstrate that *PES4* and *MIP6* share a function required for efficient sporulation.

***PES4* and *MIP6* are important for protection.** To test whether these putative RNA binding proteins have a role in protection, *pes4*Δ and *mip6*Δ strains, as well as the *pes4*Δ *mip6*Δ double mutant, were constructed in a strain background carrying an estradiol-inducible form of *NDT80*. *NDT80* is required for exit from meiotic prophase and entry into the meiotic divisions (21). In the absence of estradiol, cells arrest in meiotic prophase. Estradiol-induced transcription of *NDT80* then results in relatively synchronous passage of cells through the meiotic divisions (6, 10). The strains were placed in sporulation medium for 6 h to allow the culture to accumulate at the *ndt80* arrest point in meiotic prophase. Estradiol was then added to induce *NDT80* and allow the cells to progress into the meiotic nuclear divisions. After 2 h, part of the culture was shifted to rich medium for 1 h to allow the cells to return to mitotic growth (RTG). RNA protection was assessed using quantitative PCR (qPCR) to determine the transcript levels of three protected transcripts, *SPS4*, *SSP2*, and *GAT4*, as well as the nonprotected transcript, *SPO20*, as a control (15).

For each gene, the ratio of expression level before and after RTG 2 h after estradiol addition was measured. This "protection ratio" provides an indicator of whether the transcript was turned over upon nutrient reintroduction (i.e., was protected or not). Ratios of $\geq$1 indicate protection, and ratios of $<$1 indicate turnover. Each protected transcript exhibited a different pattern, indicating that different mRNAs have different requirements for *PES4* and *MIP6* for protection upon RTG. For example, *PES4*, but not *MIP6*, is required for protection of the *SPS4* transcript, as both the *pes4* and the *pes4 mip6* diploids exhibited very low ratios, in contrast to *mip6*Δ, which exhibited a ratio of $>$1 (Fig. 2). In contrast, *SSP2* showed a pattern more consistent with redundancy between *PES4* and *MIP6*, as both single mutants exhibited reductions in protection that were less than that observed for the double mutant (Fig. 2). For both genes, loss of protection in the *pes4*Δ *mip6*Δ double mutant was comparable to that in a *rim4* mutant. Protection of the *GAT4* transcript was reduced in the *pes4*Δ mutant but, surprisingly, not the *pes4*Δ *mip6*Δ diploid. This suggests that in the absence of *PES4* and *MIP6* some other protein may protect the *GAT4* transcript. Moreover, while *PES4* may contribute to *GAT4* protection, *MIP6* appears to interfere with protection of *GAT4* (Fig. 2). As expected, *SPO20* lacked protection in all strains. Because there is some redundancy between *PES4* and *MIP6*, the *pes4*Δ *mip6*Δ diploids were used in subsequent analyses.

***PES4* and *MIP6* are required for steady-state mRNA levels of a subset of the *NDT80* regulon.** To look more broadly at gene regulation by *PES4* and *MIP6*, a time course was performed using wild-type and *pes4*Δ *mip6*Δ *NDT80*-inducible strains. Analysis of meiotic progression indicated that wild-type and *pes4*Δ *mip6*Δ cultures entered meiosis I and meiosis II at similar times (Fig. 3A). Total mRNA was isolated from samples at 1, 2, 3, and 4 h after *NDT80* induction, and transcriptome sequencing (RNA-Seq) analysis was used to determine the RNA levels of each yeast gene. The ratios of RNA from the *pes4*Δ *mip6*Δ diploid to RNA from wild type were compared for genes of the *NDT80* regulon. A clustered heat map showed that for most genes, transcript number varied less than 4-fold up or down in the two strains, indicating that the time courses were comparable (Fig. 3B). This analysis identified a cluster of genes whose

TABLE 1 Yeast strains used in this study

Strain name	Genotype	Reference or source
AN120	*MAT***a**/*MATα ura3/ura3 his3ΔSK/his3ΔSK leu2/leu2 trp1*::*hisG/trp1*::*hisG lys2/lys2 hoΔ*::*LYS2/hoΔ*::*LYS2 arg4-NSP1/ARG1 rme1Δ*::*LEU2/RME1*	45
AN117-16D	*MAT***a** *ura3 his3ΔSK leu2 trp1*::*hisG lys2 ho*::*LYS2*	45
AN117-4B	*MATα ura3 his3ΔSK leu2 trp1*::*hisG arg4-NSP1 lys2 ho*::*LYS2 rme1*::*LEU2*	45
A14154	*MAT***a** *his3*::*hisG leu2*::*hisG trp1*::*hisG lys2 ho*::*LYS2 GAL-NDT80*::*TRP1 ura3*::p*GPD1-GAL4(848).ER*::*URA3*	14
A14155	*MATα his3*::*hisG leu2*::*hisG trp1*::*hisG lys2 ho*::*LYS2 GAL-NDT80*::*TRP1 ura3*::p*GPD1-GAL4(848).ER*::*URA3*	14
yLJ99	*MAT***a**/*MATα ura3Δ0/ura3 his3Δ1/his3 leu2Δ0/leu2 trp1*::*hisG/TRP1 met15Δ0/MET15 arg4-NSP1/ARG4 lys2/LYS2 ho*::*LYS2/ho rme1*::*LEU2/RME1 SPS4-12×MS2L/SPS4*	15
yLJ139	*MAT***a**/*MATα ura3Δ0/ura3 his3Δ1/his3 leu2Δ0/leu2 trp1*::*hisG/TRP1 met15Δ0/MET15 arg4-NSP1/ARG4 lys2/LYS2 ho*::*LYS2/ho rme1*::*LEU2/RME1 SSP2-12×MS2L/SSP2*	15
A14201	*MAT***a**/*MATα his3*::*hisG/his3*::*hisG leu2*::*hisG/leu2*::*hisG trp1*::*hisG/trp1*::*hisG lys2/lys2 ho*::*LYS2/ho*::*LYS2 GAL-NDT80*::*TRP1/GAL-NDT80*::*TRP1 ura3*::p*GPD1-GAL4(848).ER*::*URA3/ura3*::p*GPD1-GAL4(848).ER*::*URA3*	14
A31421	As 14201, plus *CLB3-3×HA*::*kanMX6/CLB3-3×HA*::*kanMX6 rim4-F349L-3×V5/rim4-F349L-3×V5*	14
yLJ80	As A14201, plus *SPS4-3HA-HIS3MX6/SPS4-3HA-HIS3MX6*	15
yLJ104	*MAT***a** *ura3Δ0 leu2Δ0 his3Δ0 trp1Δ*::*kanMX6 met15Δ0 SPS4-12×MS2L*	This study
yLJ146	As yLJ80, plus *SPR28-GFP-kanMX6/SPR28-GFP-kanMX6*	This study
yLJ178	As yKZ52, plus *SPS4-GFP-HIS3MX6/SPS4-GFP-HIS3MX6*	This study
yLJ187	As yKZ52, plus *SPR28-GFP-HIS3MX6/SPR28-GFP-HIS3MX6*	This study
yLJ189	As A14201, plus *mip6Δ*::*hphMX4/mip6Δ*::*hphMX4*	This study
yLJ190	As A14201, plus *pes4Δ*::*kanMX6/pes4Δ*::*kanMX6*	This study
yLJ197	As A14201, plus *CLB3-3HA-kanMX6/CLB3-3HA-kanMX6*	This study
yLJ199	As AN117-4B, plus *MIP6-3×sfGFP*::*kanMX6*	This study
yLJ200	As AN117-4B, plus *PES4-3×sfGFP*::*kanMX6*	This study
yLJ198	As yKZ52, plus *CLB3-3HA-kanMX6/CLB3-3HA-kanMX6*	This study
yLJ203	As AN120, plus *MIP6-3×sfGFP*::*kanMX6/MIP6*	This study
yLJ204	As AN120, plus *PES4-3×sfGFP*::*kanMX6/PES4*	This study
yLJ205	As yKZ32, plus *PES4-3×sfGFP*::*kanMX6/PES4-3×sfGFP*::*kanMX6*	This study
yLJ206	As yKZ33, plus *MIP6-3×sfGFP*::*kanMX6/MIP6-3×sfGFP*::*kanMX6*	This study
yKZ23	*MAT***a** *ura3 his3ΔSK leu2 trp1*::*hisG lys2 hoΔ*::*LYS2 mip6Δ*::*hphMX4 pes4Δ*::*kanMX6*	This study
yKZ24	*MATα ura3 leu2 his3ΔSK trp1*::*hisG lys2 hoΔ*::*LYS2 rme1Δ*::*LEU2 mip6Δ*::*hphMX4 pes4Δ*::*kanMX6*	This study
yKZ25	*MAT***a**/*MATα ura3/ura3 his3ΔSK/his3ΔSK leu2/leu2 trp1*::*hisG/trp1*::*hisG lys2/lys2 hoΔ*::*LYS2/hoΔ*::*LYS2 rme1Δ*::*LEU2/RME1 mip6Δ*::*hphMX4/mip6Δ*::*hphMX4 pes4Δ*::*kanMX6/pes4Δ*::*kanMX6*	This study
yKZ28	As AN117-16D, plus *mip6Δ*::*hphMX4*	This study
yKZ29	As AN117-4B, plus *mip6Δ*::*hphMX4*	This study
yKZ30	As AN117-16D, plus *pes4Δ*::*kanMX6*	This study
yKZ31	As AN117-4B, plus *pes4Δ*::*kanMX6*	This study
yKZ32	*MAT***a**/*MATα ura3/ura3 his3ΔSK/his3ΔSK leu2/leu2 trp1*::*hisG/trp1*::*hisG lys2/lys2 hoΔ*::*LYS2/hoΔ*::*LYS2 rme1Δ*::*LEU2/RME1 mip6Δ*::*hphMX4/mip6Δ*::*hphMX4*	This study
yKZ33	*MAT***a**/*MATα ura3/ura3 his3ΔSK/his3ΔSK leu2/leu2 trp1*::*hisG/trp1*::*hisG lys2/lys2 hoΔ*::*LYS2/hoΔ*::*LYS2 rme1Δ*::*LEU2/RME1 pes4Δ*::*kanMX6/pes4Δ*::*kanMX6*	This study
yKZ34	As yKZ23, plus *SPS4-12×MS2L*	This study
yKZ35	As yKZ23, plus *SSP2-12×MS2L*	This study
yKZ48	As A14154, plus *mip6Δ*::*hphMX4*	This study
yKZ49	As A14155, plus *mip6Δ*::*hphMX4*	This study
yKZ62	As A14154, plus *pes4Δ*::*kanMX6*	This study
yKZ63	As A14155, plus *pes4Δ*::*kanMX6*	This study
yKZ50	As A14154, plus *mip6Δ*::*hphMX4 pes4Δ*::*kanMX6*	This study
yKZ51	As A14155, plus *mip6Δ*::*hphMX4 pes4Δ*::*kanMX6*	This study
yKZ52	As A14201, plus *mip6*::*hphMX4/mip6*::*hphMX4 pes4*::*kanMX6/pes4*::*kanMX6*	This study
yKZ39	As yKZ25, plus *SPS4-12×MS2L/SPS4*	This study
yKZ40	As yKZ25, plus *SSP2-12×MS2L/SSP2*	This study
yKZ84	As yKZ52, plus *leu2*::*hisG*::*PES4*::*LEU2/leu2*::*hisG*	This study
yKZ85	As yKZ52, plus *leu2*::*hisG*::*pes4-rrm1*::*LEU2/leu2*::*hisG*	This study
yKZ86	As yKZ52, plus *leu2*::*hisG*::*pes4-rrm2*::*LEU2/leu2*::*hisG*	This study
yKZ87	As yKZ52, plus *leu2*::*hisG*::*pes4-rrm3*::*LEU2/leu2*::*hisG*	This study
yKZ91	As yKZ52, plus *leu2*::*hisG*::*LEU2/leu2*::*hisG*	This study
yKZ92	*MAT***a**/*MATα ura3/ura3Δ0 his3ΔSK/his3Δ1 leu2/leu2Δ0 trp1*::*hisG/trp1Δ*::*kanMX6 arg4-NSP1/ARG4 met15Δ0/MET15 lys2/LYS2 ho*::*LYS2/ho rme1*::*LEU2/RME1 PES4-3×sfGFP*::*kanMX6/PES4 SPS4-12×MS2L/SPS4*	This study
yKZ99	As A14201, plus *SPS4-12×MS2L/SPS4-12×MS2L*	This study
yKZ100	As A14201, plus *mip6*::*hphMX4/mip6*::*hphMX4 pes4*::*kanMX6/pes4*::*kanMX6*::*PES4-GFP*::*HIS3*	This study
yKZ101	As A14201, plus *mip6*::*hphMX4/mip6*::*hphMX4 pes4*::*kanMX6/pes4*::*kanMX6*::*pes4-rrm1-GFP*::*HIS3*	This study
yKZ102	As A14201, plus *mip6*::*hphMX4/mip6*::*hphMX4 pes4*::*kanMX6/pes4*::*kanMX6*::*pes4-rrm2-GFP*::*HIS3*	This study
yKZ103	As A14201, plus *mip6*::*hphMX4/mip6*::*hphMX4 pes4*::*kanMX6/pes4*::*kanMX6*::*pes4-rrm3-GFP*::*HIS3*	This study

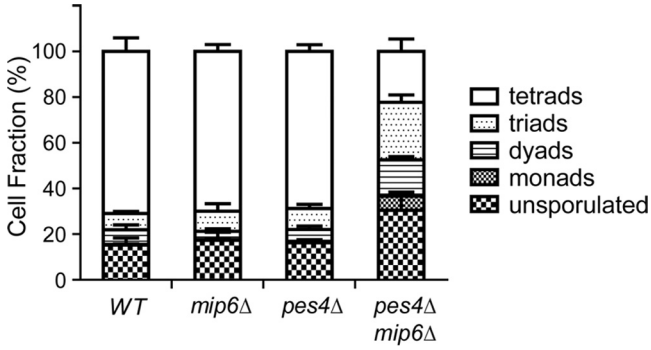

FIG 1 Sporulation in *pes4*Δ *mip6*Δ mutants. Wild-type (AN120), *mip6*Δ (yKZ32), *pes4*Δ (yKZ33), and *pes4*Δ *mip6*Δ (yKZ25) strains were sporulated, and the numbers of asci and spores per ascus were determined by light microscopy. The experiment was performed three times with 500 cells scored in each culture. Error bars indicate standard deviation (SD).

mRNA levels were downregulated at least 8-fold at at least one time point in the double mutant (Fig. 3B and C). Included in this set were nine of the 19 protected transcripts that were previously defined using microarray analysis (Fig. 3C) (15), including *SPS4* and *SSP2* but not *GAT4*. This result suggests that transcript protection and maintenance of steady-state transcript levels may be related (Fig. 3C).

***PES4* and *MIP6* are required for protection of a subset of protected transcripts.** To monitor RNA protection in the time courses shown in Fig. 3, a portion of each culture was transferred to rich medium 1, 2, and 3 h after *NDT80* induction and incubated for 1 h before collection of RNA. Of the 19 protected transcripts reported previously (15), 17 similarly displayed protection in this experiment (Fig. 4), demonstrating that the phenomenon is robust and can be reproduced using RNA-Seq.

The protection ratios of these 17 genes were then compared between wild-type and *pes4*Δ *mip6*Δ strains. Although the absolute levels of expression for several of these genes were lower in the *pes4*Δ *mip6*Δ mutant (Fig. 3), using ratios allows a comparison of the stabilities of the transcripts in wild-type and mutant strains. Twelve of the 17 genes whose transcripts were protected in the wild type exhibited a lack of protection in the *pes6*Δ *mis6*Δ diploid (Fig. 4). Consistent with the qPCR data (Fig. 2), protection of *SPS4* and *SSP2* was lost, but *GAT4* remained protected. Thus, *PES4* and/or *MIP6* is

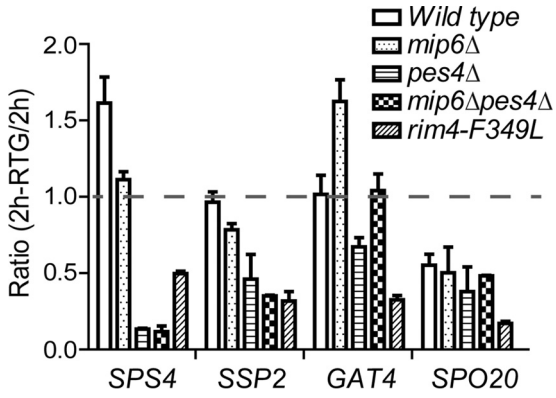

FIG 2 Protection of different mRNAs in *pes4*Δ *mip6*Δ mutants. Wild-type (A14201), *mip6*Δ (yLJ189), *pes4*Δ (yLJ190), *pes4*Δ *mip6*Δ (yKZ52), and *rim4-F349L* (A31421) strains were synchronized in sporulation using inducible *NDT80*. The levels of three protected transcripts, *SPS4*, *SSP2*, and *GAT4*, and the nonprotected transcript *SPO20* were measured by qPCR 2 h after estradiol induction and after 2 h in estradiol plus 1 additional hour after shift to rich medium. The protection ratios, i.e., the ratio of transcript levels after RTG to those before RTG, are shown. The dashed line denotes a ratio of 1, which indicates protection. Values shown are the averages from two independent experiments. Error bars indicate the range of values. Data for *rim4-F349L* are from reference 15.

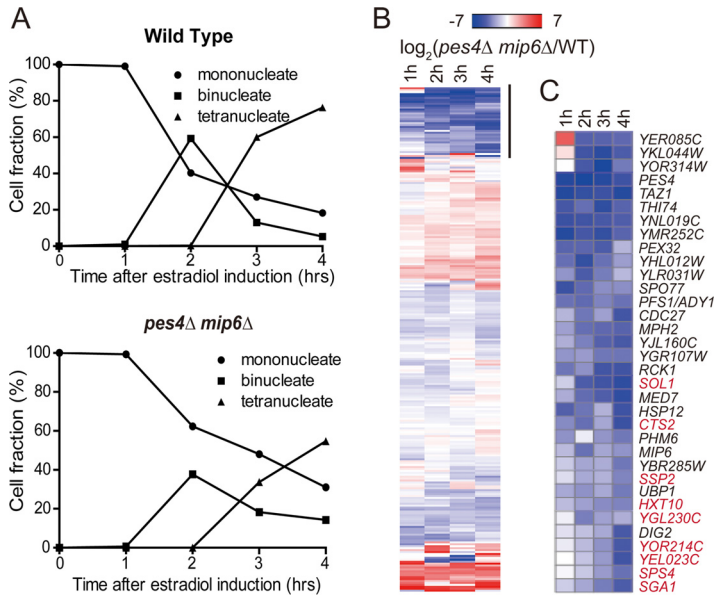

FIG 3 Induction of the *NDT80* regulon in *pes4*Δ *mip6*Δ cells. Synchronized sporulation was performed using estradiol induction of *NDT80* in wild-type (A14201) and *pes4*Δ *mip6*Δ (yKZ52) cells. Samples were removed before and at 1-h intervals after the addition of estradiol, and transcript levels were determined by RNA-Seq. (A) Meiotic progression in the two time courses as determined by DAPI staining of nuclei at each time point. (B) Heat map comparing the expression levels of genes in the *NDT80* regulon in the two strains. The $\log_2$ of the ratio of transcript levels in the *pes4*Δ *mip6*Δ strain relative to the wild type is shown. The color scale is shown for $\log_2$ of −7 to 7. The black bar indicates a cluster of genes whose expression level was reduced at least 8-fold in the *pes4*Δ *mip6*Δ strain. (C) Heat map showing the genes with reduced transcript levels in the *pes4*Δ *mip6*Δ strain indicated by the bar in panel B. Red text indicates genes previously identified as protected transcripts by RTG experiments using microarrays to measure changes in RNA levels (15). The color scale is the same as in panel B.

required for protection of a subset of the genes that exhibit protected mRNAs in the wild type.

Three classes of protected transcripts differ in their requirements for *PES4* and *MIP6*. *PES4* and *MIP6* are redundant for promoting efficient sporulation (Fig. 1). However, the qPCR analysis indicated that *PES4* was uniquely required for protection of *SPS4* and was more important than *MIP6* for the protection of *SPS2* (Fig. 2). The individual roles of *PES4* and *MIP6* in protection were determined for 11 of the 12 genes whose protection was lost in the *pes4*Δ *mip6*Δ diploid. Wild-type, *pes4*Δ, *mip6*Δ, *pes4*Δ *mip6*Δ, and *pes4*Δ *mip6*Δ/p*PES4* strains containing inducible *NDT80* were transferred to sporulation medium for 6 h, and then estradiol was added. Two hours after estradiol addition, cells were transferred to rich medium. mRNA was purified from the cells before and 1 h after RTG, and qPCR was performed to compare the expression levels of individual transcripts in the two samples. The 11 protected transcripts fell into three categories (Table 2). Class 1 behaved like *SPS4* in that *PES4* but not *MIP6* was required for protection. Three of these genes exhibited a partial suppression of the *pes4*Δ protection defect when *MIP6* was deleted, similar to what was observed for *GAT4*, although in that case the suppression was complete. Class 2 contains *SSP2* and *SPR6*, where both *PES4* and *MIP6* make independent contributions to protection (i.e., the level of protection observed for the *pes4*Δ *mip6*Δ diploid is equal to the product of the levels of the individual mutants), though the *pes4*Δ single mutant has a stronger effect, and class 3 contains genes in which each single mutant gives the same reduction in protection as the double mutant. Thus, all of the transcripts rely on *PES4* for protection, but the role of *MIP6* varies. In some instances, *MIP6* is dispensable for protection (class 1), in some it is redundant with *PES4* (class 2), and in others it is required even in the presence of *PES4* (class 3).

***PES4* and *MIP6* are required for the translational delay of *SPS4* but not *CLB3*.** Transcripts that are protected under RTG conditions also display a delay of translation

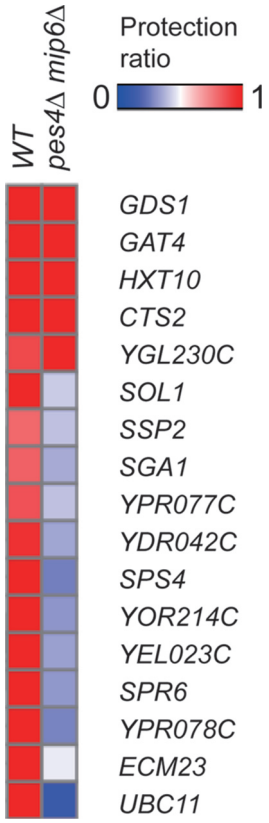

FIG 4 Effect of *pes4*Δ *mip6*Δ on protection. In the same time courses as shown in Fig. 3, samples at each time point after *NDT80* induction were transferred to rich medium for 1 h (RTG), prior to RNA isolation and RNA-Seq analysis. The heat map displays the protection ratio for 17 protected transcripts, calculated using the 2-h + 1-h RTG and 2-h time points, in the wild-type (A14201) and *pes4*Δ *mip6*Δ (yKZ52) strains.

until the end of meiosis II under normal sporulation conditions (15). Protection and late translation are genetically linked in that either inactivation of *RIM4* or hyperactivation of *IME2* eliminates both protection and late translation of *SPS4* (15). *RIM4* and *IME2* play a more general role in translational regulation as well, since the same mutants that

TABLE 2 Protection ratios in different mutants

Class and transcript	Ratio (avg ± range) for genotype[a]:				
	WT	*mip6*Δ	*pes4*Δ	*pes4*Δ *mip6*Δ	*pes4*Δ *mip6*Δ/p*PES4*
Class 1					
SPS4	**1.61 ± 0.17**	**1.11 ± 0.05**	0.13 ± 0.01	0.12 ± 0.04	**1.12 ± 0.04**
ECM23	**0.96 ± 0.05**	**0.95 ± 0.05**	0.56 ± 0.10	0.48 ± 0.11	**0.87 ± 0.06**
SOL1	**1.25 ± 0.23**	**0.96 ± 0.19**	0.21 ± 0.05	0.55 ± 0.03	**0.86 ± 0.07**
SGA1	**1.02 ± 0.09**	**0.91 ± 0.01**	0.18 ± 0.01	0.51 ± 0.07	**0.96 ± 0.10**
YEL023C	**1.01 ± 0.01**	**1.06 ± 0.07**	0.24 ± 0.07	0.48 ± 0.09	**0.92 ± 0.03**
Class 2					
SSP2	**0.96 ± 0.07**	*0.78 ± 0.04*	0.46 ± 0.16	0.35 ± 0.01	**0.89 ± 0.15**
SPR6	**1.02 ± 0.06**	*0.80 ± 0.05*	0.55 ± 0.03	0.35 ± 0.02	*0.79 ± 0.09*
Class 3					
YDR042C	**1.16 ± 0.04**	0.57 ± 0.08	0.56 ± 0.05	0.55 ± 0.05	0.50 ± 0.05
YPR078C	**1.29 ± 0.12**	0.51 ± 0.09	0.37 ± 0.05	0.53 ± 0.05	0.44 ± 0.08
YOR214C	**1.01 ± 0.04**	0.39 ± 0.07	0.62 ± 0.01	0.64 ± 0.11	0.45 ± 0.09
UBC11	**0.98 ± 0.06**	0.50 ± 0.02	0.55 ± 0.03	0.65 ± 0.10	0.57 ± 0.12

[a]Strains used were as follows: wild type, A14201; *mip6*Δ, yLJ189; *pes4*Δ, yLJ190; *pes4*Δ *mip6*Δ, yKZ52; *pes4*Δ *mip6*Δ/p*PES4*, yKZ84. Values are shown as averages from two independent experiments ± ranges. Boldface values indicate protection of the transcript. Italic values indicate intermediate transcript level.

cause early translation of *SPS4* also cause early translation of *CLB3* and other genes whose translation is normally delayed until the end of meiosis I and whose transcripts are not protected. To determine if *PES4* and *MIP6* play a role in translational regulation, proteins derived from mRNAs that are translated at different times in meiosis were epitope tagged in wild-type and *pes4*Δ *mip6*Δ *NDT80*-inducible strains and steady-state levels were examined using immunoblotting assays. The proteins analyzed were Spr28 (translated in early meiosis I), Clb3 (translated at the end of meiosis I), and Sps4 (translated at the end of meiosis II). Each of the strains was then sporulated using estradiol to synchronize the meiotic divisions, and cells were taken at various time points for protein analysis. The mitochondrial Por1 protein was used as a loading control. The experiment was performed at least three times for each strain, and a representative experiment is shown in Fig. 5. All six strains progressed through the meiotic divisions with similar kinetics (Fig. 5A), allowing us to compare the relative timing of appearance of the different proteins. In the wild-type strains, Spr28 appeared first (within an hour of *NDT80* induction), Clb3 appeared second (2 hours after *NDT80* induction), and Sps4 appeared last (2.5 h after *NDT80* induction) (Fig. 5A and B). In the *pes4*Δ *mip6*Δ background, Spr28 and Clb3 were detected with similar timing as the wild type. In contrast, Sps4 was observed at the same time as Spr28, indicating that translational delay of the *SPS4* mRNA was lost (Fig. 5A and B). The transcriptional inductions of all three genes were similar in both the wild-type and *pes4*Δ *mip6*Δ strains (Fig. 5C), confirming that these effects are posttranscriptional., *PES4* and *MIP6* promote the translational timing of only a subset of the mRNAs that are translationally controlled during sporulation by *RIM4* and *IME2*.

***PES4* and *MIP6* are required for proper localization of protected mRNAs.** Protected transcripts such as *SPS4* localize to discrete foci during sporulation. Activation of *IME2* leads to the disappearance of these foci (15). Given that Pes4 and Mip6 contain RRM domains, one possibility is that they mediate protection by sequestering RNAs. The localization of two protected transcripts, *SPS4* and *SSP2*, was therefore examined in a *pes4*Δ *mip6*Δ diploid by tagging each gene at its 3′ end with sequences encoding multiple stem-loop structures from the MS2 bacteriophage (22). Stem-loops are then formed in the 3′ UTR of the transcript, and they can be recognized by a green fluorescent protein (GFP) fusion to the MS2 coat protein expressed in the same cells. Thus, the localization of the GFP fluorescence reports on the localization of the tagged transcript (22). The *SPS4-12xMS2L* transcript displayed a protection ratio of >1 in an RTG assay, indicating that the fusion mRNA is still protected. A prospore membrane marker, Spo20$^{51\text{-}91}$-mCherry, was used to identify cells in meiosis II, so that localizations at the same stage of meiosis could be compared (23). As reported previously, both *SPS4* and *SPS2* transcripts displayed discrete puncta in wild-type cells (Fig. 6A) (15). Puncta of both transcripts were still present in the *pes4*Δ *mip6*Δ mutant cell but at lower levels (Fig. 6B). Quantification of the number of foci per cell in each strain revealed that the average number of foci per cell in the *pes4*Δ *mip6*Δ diploid dropped from 4.7 to 1 for *SPS4* and from 3.7 to 0.5 for *SSP2* (both differences, $P < 0.001$, Student's *t* test) (Fig. 6C).

One possibility is that these puncta represent a known cytoplasmic ribonucleoprotein (RNP) granule called a P-body (24). To test this, the P-body marker Edc3-mCherry (25) was coexpressed with the tagged *SPS4* mRNA. In the wild-type cells, only 7% (16/216) of the Sps4 foci displayed colocalization with the P-body marker, indicating that these foci are not P-bodies. In contrast, 91% of the Sps4 foci (64/70) remaining in the *pes4*Δ *mip6*Δ mutant colocalized with Edc3-mCherry (Fig. 6D). While the reduced number of foci in the *pes4*Δ *mip6*Δ strain could in part be due to the reduced *SPS4* transcript levels (Fig. 3), these results indicate that Pes4 and Mip6 localize the bulk of *SPS4* transcripts in foci that are not P-bodies and that loss of these proteins relocalizes the transcripts.

Pes4 and Mip6 display distinct protein localizations. Previous studies failed to detect a signal for either Pes4 or Mip6 in sporulating cells when the proteins were tagged on the C terminus with a single copy of GFP (26). The Pes4 and Mip6 proteins

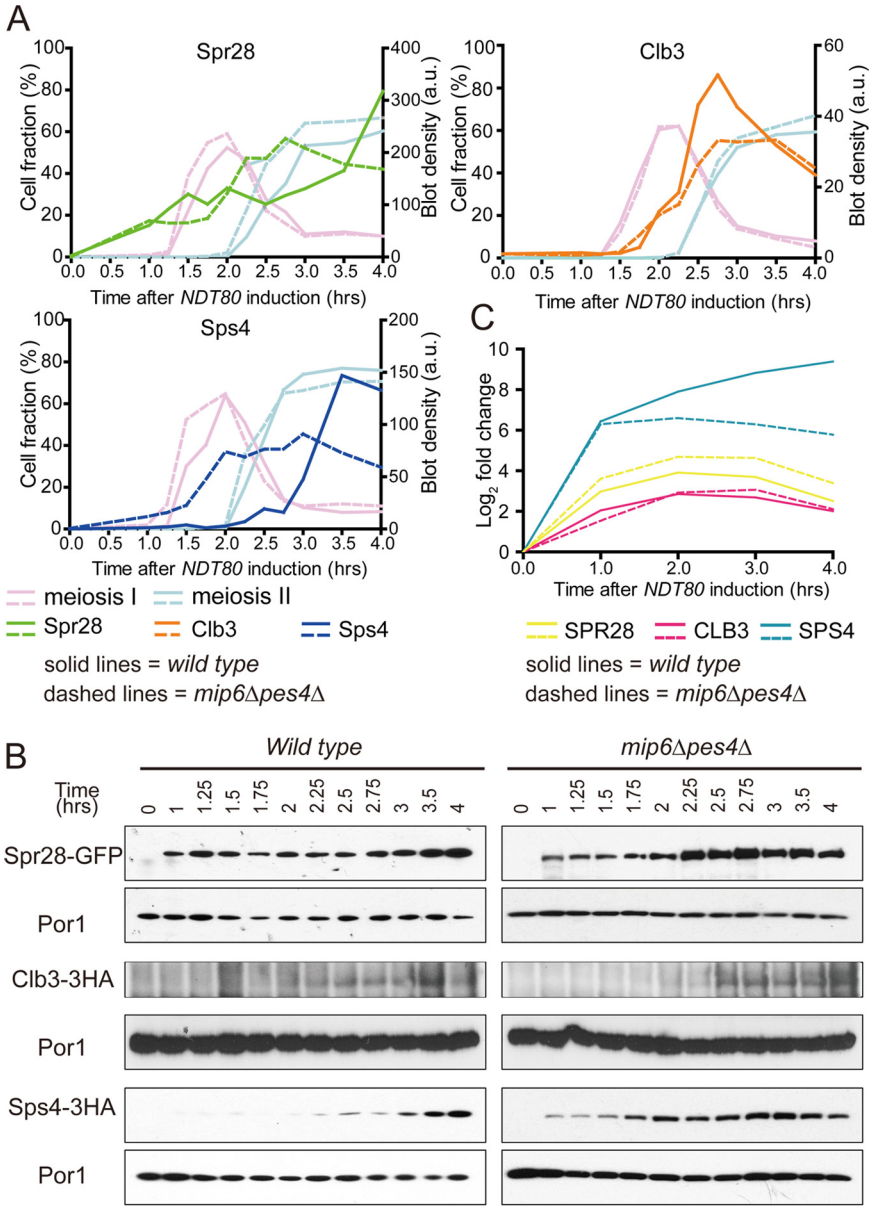

FIG 5 The timing of *SPS4* translation in *pes4*Δ *mip6*Δ cells. Wild-type and *pes4*Δ *mip6*Δ strains containing inducible *NDT80* and expressing Spr28-GFP (yLJ146 and yLJ187), Clb3-3HA (yLJ197 and yLJ198), Sps4-3HA (yLJ80), or Sps4-GFP (yLJ178) were incubated in sporulation medium for 6 h, and at the indicated times before ($t = 0$) and after estradiol addition, samples were removed and protein extracts were examined by Western blotting. (A) For each protein analyzed, meiotic progression in the wild-type and *pes4*Δ *mip6*Δ strain time courses as judged by DAPI staining is shown as well as the quantification of protein in the blots in panel B. For quantification, the density of the band for each tagged protein was normalized to the porin signal in the same lane. (B) Western blots for each protein in the different strains. The mitochondrial Por1 protein was used as a loading control. (C) The transcription of *SPR28*, *CLB3*, and *SPS4* after *NDT80* induction was examined in wild-type and *pes4*Δ *mip6*Δ strain using data from the RNA-Seq data described in the Fig. 3 legend. The *y* axis indicates the $\log_2$ of the ratio of transcript levels at each time point relative to time zero.

were observed, however, when the proteins were C-terminally tagged with three copies of GFP (3×GFP). When diploids heterozygous for *PES4-3×GFP/PES4* or *MIP6-3×GFP/MIP6* and expressing *spo20*$^{51-91}$*-mTagBFP* as a prospore membrane marker were sporulated, distinct localization patterns were observed for the two proteins (Fig. 7A). Pes4-3×GFP was found in puncta near the openings of the prospore membranes, similar to the localization pattern of the *SPS4* message, while Mip6-3×GFP localized

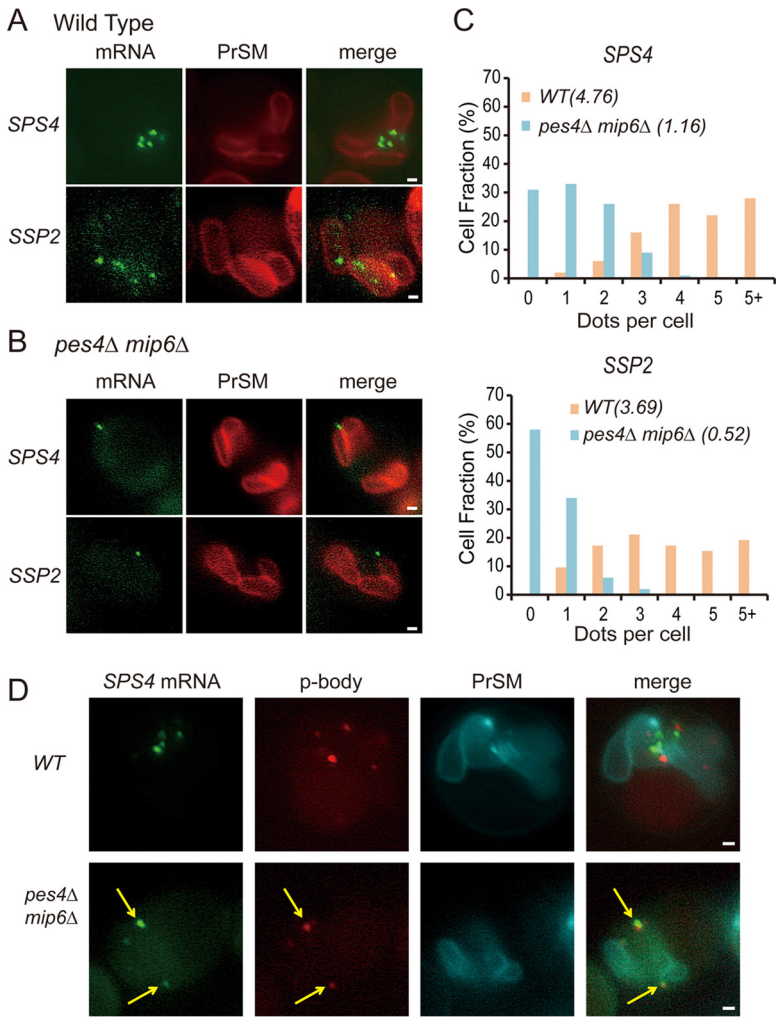

FIG 6 Localization of *SSP2* and *SPS4* transcripts in *pes4*Δ *mip6*Δ cells. (A) *SPS4::MS2L* (yLJ99) and *SSP2::MS2L* (yLJ139) strains expressing *MS2CP-GFP* and the prospore membrane marker *spo20*$^{51-91}$*-mCherry* were sporulated, and cells in mid- to late meiosis II were identified by the prospore membrane morphology. The specific mRNA localization is shown by the GFP fluorescence. (B) Localization of the *SPS4* and *SSP2* transcripts was examined in *pes4*Δ *mip6*Δ cells (yKZ39 and yKZ40) as in panel A. (C) Quantification of *SPS4* and *SSP2* transcript localization in the wild-type and *pes4*Δ *mip6*Δ cells. Graphs represent the fraction of cells with the indicated number of mRNA foci per cell. The average number of foci per cell is given in parentheses. Fifty cells were scored for each strain. (D) Colocalization of *SPS4* mRNA with the P-body in *pes4*Δ *mip6*Δ cells. Wild-type (yLJ99) and *pes4*Δ *mip6*Δ (yKZ39) *SPS4::MS2L* strains expressing *MS2CP-GFP*, the prospore membrane marker *spo20*$^{51-91}$*-mTagBFP*, and the P-body marker *EDC3-mCherry* were analyzed as in panel A. Yellow arrows indicate colocalization of the *SPS4* message with Edc3-mCherry. In wild-type cells, 7% of *SPS4* foci colocalized with Edc3-mCherry (216 foci scored in 50 cells). In the *pes4*Δ *mip6*Δ cells, 91% of *SPS4* foci displayed colocalization (70 foci scored in 50 cells). Bars, 500 nm.

along the prospore membrane in a pattern reminiscent of septin proteins (27, 28). When expressed as the only form of Pes4/Mip6 in the cell, both the Pes4- and Mip6-3×sfGFP fusions supported wild-type levels of sporulation and tetrad formation (>80% sporulation and >80% four-spored asci in both cases), indicating that the fusion proteins are functional. The distinct localizations of Pes4 and Mip6 may reflect the complex functional interaction between the two proteins.

The position of the Pes4-3×sfGFP foci in the cell is similar to foci of the *SPS4-MS2L* mRNA reporter (Fig. 6). A red fluorescent MS2 coat protein reporter (*MS2-CP-3×Red*) was constructed to allow examination of Pes4 protein and SPS4 mRNA localization in the same cells. A strain carrying *SPS4-MS2L* and *PES4-3×sfGFP* in the chromosome as well as plasmids expressing MS2-CP-3×Red and a blue fluorescent prospore membrane

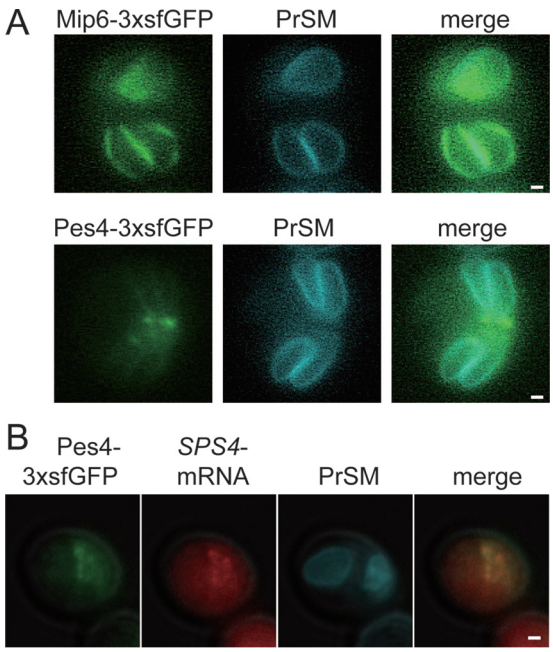

FIG 7 Localization of Pes4 and Mip6 proteins. (A) Diploid strains expressing either *MIP6-3×sfGFP* (yLJ203) or *PES4-3×sfGFP* (yLJ204) and the prospore membrane marker *spo20*$^{51-91}$*-mTagBFP* were sporulated, and cells in mid- to late meiosis II were identified by the prospore membrane morphology. (B) A strain expressing chromosomal *PES4-3×sfGFP* and *SPS4-12×MS2L* (yKZ92) was transformed with plasmids expressing *spo20*$^{51-91}$*-mTagBFP* and *MS2-CP-3×Red*. Images shown are representative of >100 cells examined for each strain. Bars, 500 nm.

marker were sporulated, and cells were observed during meiosis II. The MS2-CP-3×Red reporter gives a higher background vacuolar/cytoplasmic fluorescence than the MS2-CP-3×GFP, but of 150 cells scored that displayed discrete red foci, 100% of these foci overlapped with Pes4-3×sfGFP signal (Fig. 7B). Thus, Pes4 colocalizes with its regulatory target, the *SPS4* mRNA, in sporulating cells.

Individual RNA binding motifs of Pes4 and Mip6 are required to different extents for mRNA protection. Pes4 and Mip6 each contain three RRM domains (17). Structural studies of RRM domains have identified residues responsible for RNA binding (reviewed in reference 29). If Pes4 and Mip6 act directly on the protected transcripts, then the RNA binding motifs may be important for function. Two motifs within RRM domains, termed RNP-1 and RNP-2, are the sites of contact with the target RNA, and mutations in the RNP-1 motifs of the human TDP-43 protein and Rim4 have been shown to abrogate RNA binding and *in vivo* function, respectively (30–32). An alignment with the RRM domains of Rim4 and TDP-43 was used to identify residues in the *PES4* RRM domains in which mutations are expected to inactivate RNA binding (Fig. 8A). These mutations were introduced separately into each of the three RRM domains of *PES4*, and then plasmids carrying *PES4*, *pes4-rrm1*, *rrm-2*, and *rrm-3* alleles, as well as the vector control, were integrated into the *pes4*Δ *mip6*Δ *NDT80*-inducible strain. All of these strains were then sporulated, and protection of the seven class 1 and class 2 transcripts (Table 2) was examined by qPCR. Introduction of *PES4* complemented *pes4*Δ in the double mutant, restoring protection to *mip6*Δ levels, as expected (Table 2). A complex pattern of complementation was observed for the various *pes4-rrm* mutants (Fig. 8B). The *pes4-rrm1* allele reduced protection to a level comparable to that of *pes4*Δ for all of the transcripts except *YEL023c* and *SSP2*. The *pes4-rrm2* allele reduced protection for all the transcripts, but with a relatively modest effect on *SOL1* and *YEL023c*. The *pes4-rrm3* allele affected the protection of only two transcripts, *SGA1* and *YEL023c*. Thus, the effects of the mutations are very transcript specific. *SPS4*, *ECM23*, and *SPR6* require both RRM1 and RRM2 for protection, whereas *SSP2* requires only RRM2, *YEL023c* requires primarily RRM3, and *SGA1* requires all three RRMs. To determine if the phenotypes of the

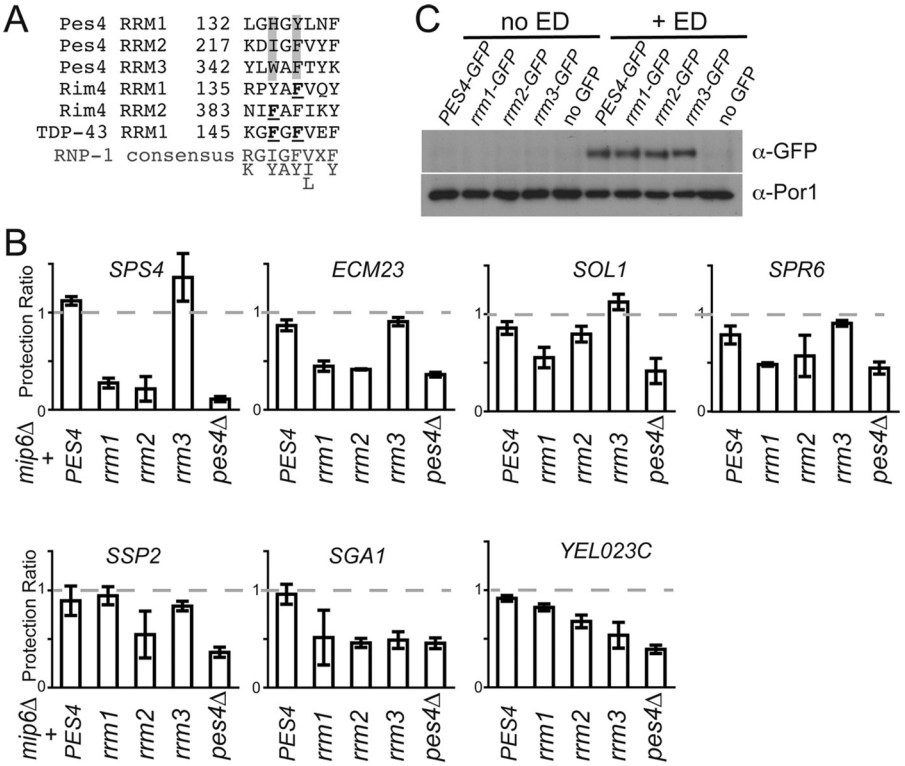

FIG 8 Requirements for individual Pes4 RRM domains for protection of different mRNAs. (A) An alignment of the RNA binding motif RNP1 (32) of the Pes4 RRM domains with the same motif in the RRM domains from Rim4 and TDP-43. Mutations of the underlined residues have been shown to inactivate Rim4 or TDP-43. Gray background indicates the residues mutated to alanine in the *pes4-rrm1*, *pes4-rrm2*, and *pes4-rrm3* alleles. The consensus for the RNP1 motif has been defined previously (32). (B) Protection in the *pes4-rrm* mutants. All seven class 1 and class 2 transcripts identified in Fig. 7 were subject to RTG 2 h after addition of estradiol and analyzed for protection by qPCR in *pes4*Δ *mip6*Δ/p*PES4* (yKZ84), *pes4*Δ *mip6*Δ/p*pes4-rrm1* (yKZ85), *pes4*Δ *mip6*Δ/p*pes4-rrm2* (yKZ86), *pes4*Δ *mip6*Δ/p*pes4-rrm3* (yKZ87), and *pes4*Δ *mip6*Δ/pRS305 (yKZ91) strains. Protection ratios shown are the averages from two independent experiments, and the error bars indicate the range. (C) Strains expressing an integrated copy of *PES4-GFP* (yKZ100), *pes4-rrm1-GFP* (yKZ101), *pes4-rrm2-GFP* (yKZ102), or *pes4-rrm3* (yKZ103) or no GFP construct (yKZ52) were transferred to sporulation medium for 6 h before addition of estradiol to induce NDT80. Cells were collected before and 3 h after estradiol addition, and the abundance of the different GFP fusions was assessed by Western blotting with anti-GFP antibodies. Antibodies to the Por1 protein were used as a loading control.

different mutants could be due to effects on protein stability, C-terminal fusions of a single GFP to the wild-type *PES4* and each of the *rrm* mutants were integrated into the *pes4*Δ *mip6*Δ *NDT80*-inducible strain and protein levels were examined by Western blotting before and after *NDT80* induction using anti-GFP antibodies (Fig. 8C). No significant differences were seen in the levels of the mutant proteins compared to Pes4. This suggests that the different phenotypes observed may be the result of changes in RNA binding rather than protein levels. In summary, the RRM domains of Pes4 are essential for protection, but which specific RRMs are necessary varies depending on the transcript.

DISCUSSION

Our earlier study led to the model that transcripts of the *NDT80* regulon whose translation is delayed until the end of meiosis II are localized into foci and that these foci serve both to sequester the transcripts away from the translational apparatus and to protect the transcripts from degradation if nutrients are reintroduced (15). The results described here are consistent with this model but reveal a more complicated and layered regulatory apparatus. In addition to the action of the Ime2 kinase and Rim4 RNA binding protein as global regulators of translational timing, other RNA binding proteins are required to "tune" the translation timing of subsets of the transcripts.

Complex functional interactions between *PES4* and *MIP6*. The effects of *PES4* and *MIP6* mutations on mRNA stability vary with the specific transcript. The mutations

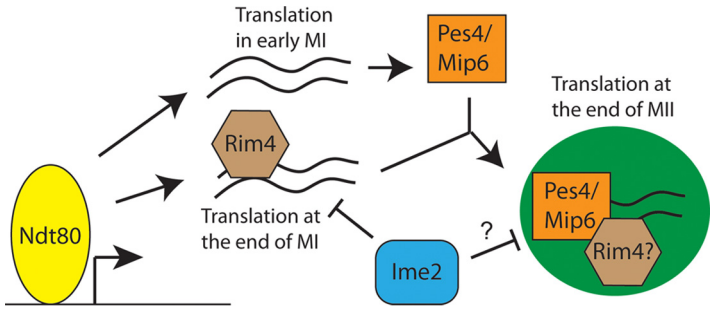

FIG 9 A translational regulatory circuit in the *NDT80* regulon. A model for the establishment of translational timing during meiosis. Ndt80 induces transcription of multiple transcripts (wavy lines). Some, including those encoding Pes4 and Mip6, are translated as soon as they are made. Others associate with the Rim4 RNA binding protein, which delays their translation. A subset of transcripts recognized by Rim4 are also recognized by Pes4 and/or Mip6, leading to their organization into foci (green circle) and further delaying their translation. Whether Rim4 remains associated with these transcripts once they are organized into foci is unclear. Ime2 acts to promote translation by antagonizing Rim4 and, possibly, Pes4/Mip6 as well.

display redundancy for protection of some transcripts, whereas other transcripts depend primarily on *PES4* with only a minor contribution from *MIP6* and still other transcripts require both genes for the protection (Table 2). Additionally, not all transcripts regulated by *PES4* and/or *MIP6* behave similarly, as the steady-state levels of ~30 transcripts are reduced during meiosis in *pes4*Δ *mip6*Δ cells but only a subset of these transcripts display protection. In contrast, for sporulation efficiency *PES4* and *MIP6* display simple redundancy. As protection correlates with late translation, one way to explain their redundancy in promoting sporulation is that either protein is able to promote the late translation or steady-state expression of one (or more) mRNA(s) that encodes a protein important for forming spores.

The effects of mutations in the RNA binding domains of *PES4* similarly vary between mRNAs as different RRM domains within Pes4 are required for protection of different transcripts. The *cis* sequences required for protection of *SPS4* have been mapped to the 5′ UTR of the transcript (15); however, sequence comparisons between the UTRs of protected transcripts have not yielded any candidate consensus sequence elements common to the different transcripts. If the different RRMs of Pes4 (or Mip6) recognize different sequences, then it may be that there is no common site in all of the transcripts.

Since Pes4 RRM domains are required for protection, it suggests that the protein interacts directly with the RNAs. Moreover, the localization of Pes4 overlaps with that of the *SPS4* message, consistent with the possibility that Pes4 binds to the *SPS4* transcript. However, direct binding of Pes4 or Mip6 to its regulatory targets has not yet been demonstrated.

The differing localizations of Pes4 and Mip6 support the conclusion that the proteins are not simply redundant. One interesting question is whether the localization of Pes4 and Mip6 is linked to the ultimate localization of the proteins whose transcripts they regulate. For example, the localization of Pes4 foci outside the prospore membranes suggests that any transcripts associated with Pes4, and the proteins translated from them, would end up primarily in the ascus and excluded from the spores. In contrast, association with Mip6 might lead to translation primarily within the spore cytoplasm. Consistent with this, *SPS4*, which is most clearly dependent on *PES4* and independent of *MIP6* (Table 2), is found primarily on lipid droplets that are in the ascal cytoplasm (20, 26), but whether this is related to localization of the transcript requires further investigation.

Model for timing of translational regulation in sporulation. A model incorporating Pes4 and Mip6 into the *IME2*- and *RIM4*-dependent pathway for regulating translation timing during sporulation is shown in Fig. 9. Activation of Ndt80 leads to the production of multiple transcripts that can be separated by their translational timing. Transcripts whose translation will be delayed associate with Rim4 (14). Pes4 and Mip6 are among the proteins translated as soon as their mRNAs are transcribed. These

proteins bind to a subset of the Rim4-associated mRNAs and sequester them into foci. Sequestration in foci both causes a further translational delay and protects these specific transcripts from degradation when cells are returned to nutrient-rich medium. Whether Rim4 remains associated with the transcripts in these foci, as shown in the model, or there is some "handoff" from Rim4 to Pes4/Mip6 is as yet unknown. Localization of Rim4 indicates that the protein is not localized in foci as seen for Pes4 (33) (Fig. 8). However, it may be that there is a small, cytologically undetectable fraction of Rim4 present in these foci. Ime2 acts as an inhibitor of Rim4, and constitutive activation of Ime2 eliminates protection, translational delay, and focal localization of the *SPS4* transcript (14, 15). Whether these effects of Ime2 are mediated through its activity on Rim4 or whether it independently targets Pes4 or Mip6 needs to be investigated.

A conserved regulatory circuit in gametogenesis. The mRNAs for *PES4* and *MIP6* and their regulatory targets are all induced by *NDT80*. Thus, *NDT80* upregulates expression of both the late translated genes and the means to delay their translation. In this way, a coarse transcriptional regulatory program establishes a more fine-tuned translational timing. These results have an interesting parallel in the regulation of meiotic gene expression in the fission yeast, *Schizosaccharomyces pombe*. In fission yeast, the transcription factor Mei4 plays a role analogous to Ndt80, causing the upregulation of genes required for both the meiotic divisions and spore packaging (34, 35). Included in the Mei4 regulon is the RRM-containing protein Meu5 (36). A coprecipitation analysis revealed that Meu5 binds to a set of other Mei4-induced messages and that the steady-state level of these transcripts is lowered in a *meu5* mutant strain (36). This provides a parallel with *MIP6*/*PES4*, in which a subset of the transcripts of the *NDT80* regulon is reduced in the mutant, though there is not yet direct evidence that Pes4/Mip6 bind these mRNAs. The analogy between the two systems can be extended, as a ribosome profiling study of translational timing in *S. pombe* meiosis revealed a class of transcripts whose translational efficiency is increased later in meiosis, consistent with a delayed translation (37). This class is enriched in Meu5 target mRNAs (37), suggesting that Meu5 binding might promote delayed translation, again parallel to the situation in budding yeast. Though *meu5* is not an ortholog of *MIP6*/*PES4*, like the *Saccharomyces cerevisiae* proteins it contains three RRM domains. It will be of interest to learn if Meu5 controls the localization as well as abundance and translation of its target mRNAs.

These observations suggest that, though the factors are different, the same regulatory logic to convert timing of gene expression from transcriptional control to translational control is present in both yeasts. Interestingly, in mammalian spermatogenesis, the chromatoid body, an RNP particle formed early in meiosis, has been suggested to sequester mRNAs for translation later during sperm differentiation. It may be that this translational timing regulatory circuit is a conserved strategy for the developmental timing of gene expression during gametogenesis.

MATERIALS AND METHODS

Yeast media, strains, and plasmids. Unless otherwise noted, standard media and growth conditions were used (38). All yeast strains used in this study are in the SK1 background and are listed in Table 1. To create the diploid strains yLJ189 and yLJ190, the open reading frame (ORF) of *MIP6* or *PES4* was replaced with *hphMX4* and *kanMX6* (39, 40), respectively, by PCR-based integration in the haploid strains A14154 and A14155. The resulting haploids yKZ48, yKZ49, yKZ62, and yKZ63 were then mated to create the diploids. The *pes4*Δ *mip6*Δ haploids, yKZ50 and yKZ51, are segregants from a cross of yKZ48 and yKZ63. yKZ50 and yKZ51 were mated to produce yKZ52. *MIP6* and *PES4* were similarly deleted from the haploid strains AN117-16D and AN117-4B, to generate yKZ28, yKZ29, yKZ30, and yKZ31, and the appropriate haploids were mated to generate the diploids yKZ32 and yKZ33. yKZ23 and yKZ24 are segregants from a cross of yKZ28 and yKZ31, which were mated to produce yKZ25. To make the diploid strains yLJ146, yLJ178, yLJ187, yLJ197, and yJL198, which carry homozygous 3× hemagglutinin (HA) or green fluorescent protein (GFP) tags fused to *SPR28*, *SPS4*, or *CLB3*, the appropriate gene was tagged by PCR-based integration by first amplifying fragments containing the tag and a selectable marker using pFA6a-3HA-kanMX6, pFA6a-GFP(S65T)-HIS3MX6, or pFA6a-GFP(S65T)-kanMX6 (40). These fragments were transformed into the wild-type (WT) haploids A14154 and A14155 or the *mip6*Δ *pes4*Δ haploids yKZ50 and yKZ51, and the resulting haploids were mated to create diploid strains. All deletion and tagged alleles were confirmed by colony PCR. To make yLJ203 and yLJ204, *3×Superfolder GFP* (*sfGFP*; a gift of G. Zhao) was integrated at the 3′ end of *MIP6* or *PES4* in AN117-4B, creating yLJ199 and yLJ200, respectively, and then mated with AN117-16D. Strains yLJ205 and yLJ206, used to test the functionality

of the 3×sf-GFP-tagged Pes4 and Mip6, were constructed by PCR-mediated tagging of *PES4* and *MIP6* at their 3′ ends with *3×sfGFP* in strains yKZ32 and yKZ33, respectively. These diploids were then dissected, and appropriate segregants were mated to create yLJ205 and yLJ206. To place MS2 loops in the 3′ UTR of *SPS4* or *SSP2* in *mip6*Δ *pes4*Δ strains, a *GFP-HIS3MX6* cassette was first introduced into yKZ23 at the 3′ end of each gene by PCR-based integration and then replaced with MS2 loops by CRISPR-Cas9 (clustered regularly interspaced short palindromic repeat)-mediated recombination as described in reference 15, creating yKZ34 and yKZ35, which were then mated to yKZ24 to generate diploid strains yKZ39 and yKZ40, respectively. Strain yKZ99, used to test protection of the *SPS4-12×MS2L* fusion, was constructed by CRISPR-Cas9-mediated replacement of a *3×HA-HIS3MX6* tag on *SPS4* in strains yLJ76 and yLJ77 (15) with a 12×MS2L sequence. The resulting strains were mated to create yKZ99. To create strain yKZ92, the *TRP1* gene in yLJ97 (15) was replaced with the *kanMX6* cassette by PCR-mediated integration, creating yLJ104, and yLJ104 was then crossed with yLJ200.

To construct the integration plasmid carrying wild-type *PES4*, the *PES4* ORF with 608 nucleotides of upstream sequence and 304 nucleotides of downstream sequence was amplified using PCR with genomic SK1 DNA as the template and assembled into the XbaI/XhoI-digested yeast integration plasmid pRS305 (41) using the GeneArt seamless cloning and assembly kit (Invitrogen), creating pKZ59. Integrating plasmids carrying the *pes4-H134A Y136A* (designated *pes4-rrm1*), *pes4-I219A F221A* (*pes4-rrm2*), and *pes4-W344 AF346A* (*pes4-rrm3*) alleles were generated by amplifying the *PES4* region carried in pKZ59 in two pieces with overlapping oligonucleotides that carried the point mutations. In each case, these two pieces were combined with XbaI/XhoI-digested pRS305 plasmid and assembled using GeneArt seamless cloning, creating pKZ60 (*pes4-rrm1*), pKZ61 (*pes4-rrm2*), and pKZ62 (*pes4-rrm3*). The presence of the mutations, and the absence of any unexpected mutations, was confirmed by sequencing by the Stony Brook University DNA Sequencing Facility. These plasmids, and the empty vector pRS305, were linearized by digestion with AflII prior to transformation into yKZ52, to generate strains yKZ84, yKZ85, yKZ86, yKZ87, and yKZ91. To examine levels of the mutant proteins, *PES4* and the three *rrm* alleles were each tagged with a single copy of *GFP* at the 3′ end. The coding region and 608 bp of the promoter of the *PES4* gene (or the appropriate *rrm* mutant) were amplified by PCR. A fragment carrying the coding region of GFP and the *ADH1* terminator was amplified from pFA6a-GFP(S65T) (40), and the two PCR products were combined with XbaI-XhoI-cut pRS305 using the Gene Art assembly kit. The resulting plasmids, pKZ76 (*PES4-GFP*), pKZ77 (*pes4-rrm1-GFP*), pKZ78 (*pes4-rrm2-GFP*), and pKZ79 (*pes4-rrm3-GFP*), were digested with Bsu361 to target integration to the *PES4* promoter and transformed into yKZ52, producing strains yKZ100 to yKZ103, respectively. For fluorescence experiments, plasmid pMS2-CP-3xGFP (22) was used to identify the localization of tagged mRNAs. pRS426-*spo20*$^{51-91}$*-mCherry* (23) or pRS426-*spo20*$^{51-91}$*-mTagBFP* (20) was used to visualize the prospore membranes, and pRP1574 (Edc3-mCherry) (25) was used to label P-bodies. The plasmid encoding a red fluorescent version of the MS2 coat protein, pKZ51, was constructed by digesting pMS2-CP-3xGFP with BamHI and EagI to remove both the GFP sequences and the *CYC1* terminator and inserting an *S. cerevisiae* codon-optimized version of *mOrange* and the *ADH1* terminator using Gibson assembly. The resulting plasmid was digested with PacI, and *mCherry* was then inserted in frame between the coat protein coding sequence and *mOrange* via Gibson assembly. Finally, this vector digested with PacI and SpeI and a similarly digested fragment carrying *mRFP* were inserted. The final construct contains the MS2 coat protein fused in frame with mRFP-mCherry-mOrange and is referred to as MS2-CP-3×Red.

Sporulation and RTG conditions. To sporulate yeast strains containing an inducible version of *NDT80* (P_{GAL}*-NDT80* combined with *GAL4-ER*) (6), cells were grown in liquid yeast extract-peptone-dextrose (YPD) medium overnight at 30°C and then diluted into liquid yeast extract-peptone-potassium acetate (YPA) medium to 2×10^6 cells/ml. Cells were incubated on a shaker at 30°C until the culture reached a concentration of 2×10^7 cells/ml (about 18 h) and then were washed with distilled water (dH_2O), resuspended in sporulation medium (SPM; 2% potassium acetate) at 3×10^7 cells/ml, and incubated at 30°C for 6 h to allow cells to proceed through DNA replication and arrest in meiotic prophase. β-Estradiol was then added to the culture to a final concentration of 1 μM to induce expression of *NDT80* and entry into the meiotic divisions. For return-to-growth (RTG) experiments, cells at each time point were washed once with dH_2O, resuspended in twice the volume of YPD medium, and incubated at 30°C. To harvest cells for expression analysis, cells were pelleted, washed once with dH_2O, and flash frozen in liquid nitrogen. To determine the stage of meiosis, 90 μl cells was fixed by addition of 10 μl 37% formaldehyde. DNA of fixed cells was stained with 4′,6-diamidino-2-phenylindole (DAPI), and the nuclei were counted using a Zeiss Axioplan 2 microscope. At least 300 cells were counted for each sample.

mRNA localization. To observe the localization of MS2 loop-tagged transcripts, strains yKZ39 and yKZ40 carrying p*MS2-CP-GFP* along with either pRS426-*spo20*$^{51-91}$*-mCherry* or both pRS426-*spo20*$^{51-91}$*-mTagBFP* and pRP1574 (*EDC3-mCherry*) were incubated in SD-His-Trp-Ura liquid medium overnight at 30°C and diluted in YPA to 2.5×10^6 cells/ml. After incubation overnight at 30°C, the cells were washed with dH_2O, resuspended in SPM at a concentration of 2×10^7 cells/ml, and incubated at 30°C for 5 to 6 h. Samples were then placed on microscope slides and observed using a Zeiss Axioplan 2 microscope, and images were taken by a Zeiss mRM digital camera and processed with AxioVision 4.0 software.

Immunoblot assays. To detect Sps4 and Spr28 by immunoblot analysis, 5 ml of cell culture was collected at various times during the sporulation time courses. Cell pellets were resuspended in a 1:1 volume of 5% trichloroacetic acid (TCA) and incubated at 4°C for 10 min. Cells were pelleted again by spinning for 3 min at 1,000 × *g*, washed once in 1 ml acetone, spun at 16,000 × *g* for 5 min, and allowed to air dry for 2.5 to 3 h. Dried pellets were suspended in 100 μl freshly prepared lysis buffer (50 mM Tris, pH 7.5, 1 mM EDTA, 27.5 mM dithiothreitol [DTT], 11 mM phenylmethylsulfonyl fluoride [PMSF], 2× concentrated EDTA-free complete protease inhibitor cocktail tablets [Roche]). Cells were lysed by addition of 50 μl zirconia beads followed by bead-beating twice at 6 m/s for 40 s with a FastPrep 24

high-speed benchtop homogenizer (MP Biomedicals) with the cells kept on ice between bead beatings. Fifty microliters 3× sodium dodecyl sulfate (SDS) sample buffer was added to each lysate, and the protein samples were boiled for 5 min before loading onto a 10% SDS polyacrylamide gel. To detect Clb3, 10 ml of cell culture was collected, resuspended in 20% TCA, spun at 1,000 × *g* for 3 min, and resuspended in 400 μl 20% TCA. Cells were lysed by addition of 400 μl zirconia beads followed by bead beating twice at 6 m/s for 40 s with a FastPrep 24 high-speed benchtop homogenizer (MP Biomedicals). The lysates were collected and pelleted, and the pellets were then washed with 1 ml cold acetone and allowed to air dry for 2.5 to 3 h. The dried pellets were resuspended in 100 μl buffer (100 mM Tris-HCl, pH 8.8, 6 M urea, 10 mM EDTA, 1% SDS, and 0.4 M NaCl) and incubated at 30°C for 1 h on a rotator. Cell debris was removed by centrifugation at 16,000 × *g* for 10 min, and then SDS sample buffer was added to the supernatants and boiled for 5 min before loading onto a 10% SDS polyacrylamide gel. Wet transfer onto a polyvinylidene difluoride (PVDF) membrane (Bio-Rad) was performed using a mini-Transblot cell (Bio-Rad). Sps4-GFP and Spr28-GFP were detected using monoclonal anti-GFP antibodies (Clontech) at 1:1,000 dilution. Sps4-3HA and Clb3-3HA were detected by using monoclonal anti-HA antibodies (Sigma) at 1:1,000 dilution. As a loading control, porin was detected using monoclonal anti-Por1 antibodies (Molecular Probes). Horseradish peroxidase (HRP)-conjugated anti-mouse antibodies (Amersham Biosciences) were used at 1:5,000 dilution for detection of the HA and GFP epitopes and 1:15,000 for detection of porin, and proteins were detected using Clarity-Western ECL substrate (Bio-Rad). Quantification was performed using the ImageJ software. All time courses and Western blot assays were performed twice, and a representative time course is shown in Fig. 5. For analysis of the Pes4-GFP fusion proteins, cells were collected before and 3 h after addition of estradiol to the culture medium. Cells were prepared and samples were analyzed as described above for the Sps4-GFP and Spr28-GFP fusions.

qPCR assays. Cells from 5 ml of culture taken at various time points were collected by centrifugation, and total mRNA was extracted and purified with a RiboPure yeast kit (Ambion). cDNA was synthesized from the mRNA using the qScript cDNA SuperMix (Quanta Bioscience) and then treated with RNase A (0.5 μg/μl) at 37°C for 30 min. The cDNA was then purified using a PCR purification kit (Qiagen). The cDNA concentration was measured using a NanoDrop spectrophotometer (Thermo Scientific) and adjusted to 1 ng/μl for quantitative PCRs. mRNA levels for each gene were determined by qPCR using a Mastercycler EP Realplex (Eppendorf) and LightCycler 480 DNA Sybr green I PCR master mix (Roche). All samples were assayed in triplicate, and all experiments have been performed at least twice.

RNA-Seq and analysis. Total RNA was extracted and purified from 5 ml of sporulating culture at various time points using the RiboPure yeast kit (Ambion). cDNA synthesis and library preparation were performed using the Ovation universal RNA-Seq system (NuGEN). Libraries were pooled and run together on the Illumina MiSeq platform using MiSeq reagent kit v3 (Illumina). Reads were aligned to yeast reference genome *Saccharomyces cerevisiae* S288C R64.1.1 with Bowtie2 v.2.2.7 (42). The output sequence alignment/map (SAM) files were sorted and converted to binary (BAM) files using SAMtools v.1.3.1 (43). Fragments per kilobase of transcript per million mapped reads (FPKMs) were then calculated using Cufflinks v.2.2.1 (44). Clustering was performed, and heat maps were created using GENE-E (http://www.broadinstitute.org/cancer/software/GENE-E/).

ACKNOWLEDGMENTS

We thank Gang Zhao, Bruce Futcher, Jeffery Gerst, and Angelika Amon for strains and plasmids. We are grateful to Hong Wang and the Yeast Center Microarray Facility for assistance with library construction and cDNA sequencing, Nancy Hollingsworth for comments on the manuscript, and members of the Neiman and Futcher labs for helpful discussions.

This work was supported by P01 GM088297 to R.S. and A.M.N. and NIH grant R01 GM072540 to A.M.N.

REFERENCES

1. Neiman AM. 2011. Sporulation in the budding yeast *Saccharomyces cerevisiae*. Genetics 189:737–765. https://doi.org/10.1534/genetics.111.127126.
2. Neiman AM. 1998. Prospore membrane formation defines a developmentally regulated branch of the secretory pathway in yeast. J Cell Biol 140:29–37. https://doi.org/10.1083/jcb.140.1.29.
3. Lynn RR, Magee PT. 1970. Development of the spore wall during ascospore formation in *Saccharomyces cerevisiae*. J Cell Biol 44:688–692. https://doi.org/10.1083/jcb.44.3.688.
4. Kassir Y, Granot D, Simchen G. 1988. *IME1*, a positive regulator gene of meiosis in *S. cerevisiae*. Cell 52:853–862. https://doi.org/10.1016/0092-8674(88)90427-8.
5. Smith HE, Mitchell AP. 1989. A transcriptional cascade governs entry into meiosis in *Saccharomyces cerevisiae*. Mol Cell Biol 9:2142–2152. https://doi.org/10.1128/MCB.9.5.2142.
6. Benjamin KR, Zhang C, Shokat KM, Herskowitz I. 2003. Control of landmark events in meiosis by the CDK Cdc28 and the meiosis-specific kinase Ime2. Genes Dev 17:1524–1539. https://doi.org/10.1101/gad.1101503.
7. Chu S, Herskowitz I. 1998. Gametogenesis in yeast is regulated by a transcriptional cascade dependent on Ndt80. Mol Cell 1:685–696. https://doi.org/10.1016/S1097-2765(00)80068-4.
8. Winter E. 2012. The Sum1/Ndt80 transcriptional switch and commitment to meiosis in *Saccharomyces cerevisiae*. Microbiol Mol Biol Rev 76:1–15. https://doi.org/10.1128/MMBR.05010-11.
9. Chu S, DeRisi J, Eisen M, Mulholland J, Botstein D, Brown PO, Herskowitz I. 1998. The transcriptional program of sporulation in budding yeast. Science 282:699–705. https://doi.org/10.1126/science.282.5389.699.
10. Carlile TM, Amon A. 2008. Meiosis I is established through division-specific translational control of a cyclin. Cell 133:280–291. https://doi.org/10.1016/j.cell.2008.02.032.
11. Coluccio A, Bogengruber E, Conrad MN, Dresser ME, Briza P, Neiman AM. 2004. Morphogenetic pathway of spore wall assembly in *Saccharomyces cerevisiae*. Eukaryot Cell 3:1464–1475. https://doi.org/10.1128/EC.3.6.1464-1475.2004.
12. Sourirajan A, Lichten M. 2008. Polo-like kinase Cdc5 drives exit from

pachytene during budding yeast meiosis. Genes Dev 22:2627–2632. https://doi.org/10.1101/gad.1711408.
13. Brar GA, Yassour M, Friedman N, Regev A, Ingolia NT, Weissman JS. 2012. High-resolution view of the yeast meiotic program revealed by ribosome profiling. Science 335:552–557. https://doi.org/10.1126/science.1215110.
14. Berchowitz LE, Gajadhar AS, van Werven FJ, De Rosa AA, Samoylova ML, Brar GA, Xu Y, Xiao C, Futcher B, Weissman JS, White FM, Amon A. 2013. A developmentally regulated translational control pathway establishes the meiotic chromosome segregation pattern. Genes Dev 27:2147–2163. https://doi.org/10.1101/gad.224253.113.
15. Jin L, Zhang K, Xu Y, Sternglanz R, Neiman AM. 2015. Sequestration of mRNAs modulates the timing of translation during meiosis in budding yeast. Mol Cell Biol 35:3448–3458. https://doi.org/10.1128/MCB.00189-15.
16. Friedlander G, Joseph-Strauss D, Carmi M, Zenvirth D, Simchen G, Barkai N. 2006. Modulation of the transcription regulatory program in yeast cells committed to sporulation. Genome Biol 7:R20. https://doi.org/10.1186/gb-2006-7-3-r20.
17. Query CC, Bentley RC, Keene JD. 1989. A common RNA recognition motif identified within a defined U1 RNA binding domain of the 70K U1 snRNP protein. Cell 57:89–101. https://doi.org/10.1016/0092-8674(89)90175-X.
18. Byrne KP, Wolfe KH. 2005. The Yeast Gene Order Browser: combining curated homology and syntenic context reveals gene fate in polyploid species. Genome Res 15:1456–1461. https://doi.org/10.1101/gr.3672305.
19. Wolfe KH, Shields DC. 1997. Molecular evidence for an ancient duplication of the entire yeast genome. Nature 387:708–713. https://doi.org/10.1038/42711.
20. Lin CP, Kim C, Smith SO, Neiman AM. 2013. A highly redundant gene network controls assembly of the outer spore wall in *S. cerevisiae*. PLoS Genet 9:e1003700. https://doi.org/10.1371/journal.pgen.1003700.
21. Xu L, Ajimura M, Padmore R, Klein C, Kleckner N. 1995. *NDT80*, a meiosis-specific gene required for exit from pachytene in *Saccharomyces cerevisiae*. Mol Cell Biol 15:6572–6581. https://doi.org/10.1128/MCB.15.12.6572.
22. Haim-Vilmovsky L, Gerst JE. 2009. m-TAG: a PCR-based genomic integration method to visualize the localization of specific endogenous mRNAs in vivo in yeast. Nat Protoc 4:1274–1284. https://doi.org/10.1038/nprot.2009.115.
23. Suda Y, Nakanishi H, Mathieson EM, Neiman AM. 2007. Alternative modes of organellar segregation during sporulation in *Saccharomyces cerevisiae*. Eukaryot Cell 6:2009–2017. https://doi.org/10.1128/EC.00238-07.
24. Parker R, Sheth U. 2007. P bodies and the control of mRNA translation and degradation. Mol Cell 25:635–646. https://doi.org/10.1016/j.molcel.2007.02.011.
25. Buchan JR, Muhlrad D, Parker R. 2008. P bodies promote stress granule assembly in *Saccharomyces cerevisiae*. J Cell Biol 183:441–455. https://doi.org/10.1083/jcb.200807043.
26. Lam C, Santore E, Lavoie E, Needleman L, Fiacco N, Kim C, Neiman AM. 2014. A visual screen of protein localization during sporulation identifies new components of prospore membrane-associated complexes in budding yeast. Eukaryot Cell 13:383–391. https://doi.org/10.1128/EC.00333-13.
27. De Virgilio C, DeMarini DJ, Pringle JR. 1996. *SPR28*, a sixth member of the septin gene family in *Saccharomyces cerevisiae* that is expressed specifically in sporulating cells. Microbiology 142:2897–2905. https://doi.org/10.1099/13500872-142-10-2897.
28. Fares H, Goetsch L, Pringle JR. 1996. Identification of a developmentally regulated septin and involvement of the septins in spore formation in *Saccharomyces cerevisiae*. J Cell Biol 132:399–411. https://doi.org/10.1083/jcb.132.3.399.
29. Maris C, Dominguez C, Allain FH. 2005. The RNA recognition motif, a plastic RNA-binding platform to regulate post-transcriptional gene expression. FEBS J 272:2118–2131. https://doi.org/10.1111/j.1742-4658.2005.04653.x.
30. Kuo PH, Chiang CH, Wang YT, Doudeva LG, Yuan HS. 2014. The crystal structure of TDP-43 RRM1-DNA complex reveals the specific recognition for UG- and TG-rich nucleic acids. Nucleic Acids Res 42:4712–4722. https://doi.org/10.1093/nar/gkt1407.
31. Soushko M, Mitchell AP. 2000. An RNA-binding protein homologue that promotes sporulation-specific gene expression in *Saccharomyces cerevisiae*. Yeast 16:631–639.
32. Kramer K, Sachsenberg T, Beckmann BM, Qamar S, Boon KL, Hentze MW, Kohlbacher O, Urlaub H. 2014. Photo-cross-linking and high-resolution mass spectrometry for assignment of RNA-binding sites in RNA-binding proteins. Nat Methods 11:1064–1070. https://doi.org/10.1038/nmeth.3092.
33. Berchowitz LE, Kabachinski G, Walker MR, Carlile TM, Gilbert WV, Schwartz TU, Amon A. 2015. Regulated formation of an amyloid-like translational repressor governs gametogenesis. Cell 163:406–418. https://doi.org/10.1016/j.cell.2015.08.060.
34. Horie S, Watanabe Y, Tanaka K, Nishiwaki S, Fujioka H, Abe H, Yamamoto M, Shimoda C. 1998. The *Schizosaccharomyces pombe mei4*+ gene encodes a meiosis-specific transcription factor containing a forkhead DNA-binding domain. Mol Cell Biol 18:2118–2129. https://doi.org/10.1128/MCB.18.4.2118.
35. Mata J, Lyne R, Burns G, Bahler J. 2002. The transcriptional program of meiosis and sporulation in fission yeast. Nat Genet 32:143–147. https://doi.org/10.1038/ng951.
36. Amorim MJ, Cotobal C, Duncan C, Mata J. 2010. Global coordination of transcriptional control and mRNA decay during cellular differentiation. Mol Syst Biol 6:380. https://doi.org/10.1038/msb.2010.38.
37. Duncan CD, Mata J. 2014. The translational landscape of fission-yeast meiosis and sporulation. Nat Struct Mol Biol 21:641–647. https://doi.org/10.1038/nsmb.2843.
38. Rose MD, Fink GR. 1990. Methods in yeast genetics. Cold Spring Harbor Laboratory Press, Cold Spring Harbor, NY.
39. Goldstein AL, McCusker JH. 1999. Three new dominant drug resistance cassettes for gene disruption in *Saccharomyces cerevisiae*. Yeast 15:1541–1553.
40. Longtine MS, McKenzie A, III, Demarini DJ, Shah NG, Wach A, Brachat A, Philippsen P, Pringle JR. 1998. Additional modules for versatile and economical PCR-based gene deletion and modification in *Saccharomyces cerevisiae*. Yeast 14:953–961.
41. Sikorski RS, Hieter P. 1989. A system of shuttle vectors and yeast host strains designed for efficient manipulation of DNA in *Saccharomyces cerevisiae*. Genetics 122:19–27.
42. Langmead B, Salzberg SL. 2012. Fast gapped-read alignment with Bowtie 2. Nat Methods 9:357–359. https://doi.org/10.1038/nmeth.1923.
43. Li H, Handsaker B, Wysoker A, Fennell T, Ruan J, Homer N, Marth G, Abecasis G, Durbin R, 1000 Genome Project Data Processing Subgroup. 2009. The Sequence Alignment/Map format and SAMtools. Bioinformatics 25:2078–2079. https://doi.org/10.1093/bioinformatics/btp352.
44. Trapnell C, Williams BA, Pertea G, Mortazavi A, Kwan G, van Baren MJ, Salzberg SL, Wold BJ, Pachter L. 2010. Transcript assembly and quantification by RNA-Seq reveals unannotated transcripts and isoform switching during cell differentiation. Nat Biotechnol 28:511–515. https://doi.org/10.1038/nbt.1621.
45. Neiman AM, Katz L, Brennwald PJ. 2000. Identification of domains required for developmentally regulated SNARE function in *Saccharomyces cerevisiae*. Genetics 155:1643–1655.